Solar still performance and enhancement techniques analysis using an alternative thermal model approach

André António Vieira Lisboa
andre.lisboa@tecnico.ulisboa.pt

Instituto Superior Técnico, Universidade de Lisboa, Portugal

January 2021

Abstract

Around the globe, increasing water stress and scarcity are becoming a problem that particularly affects developing regions. A viable solution for coastal areas can be the desalination of seawater. It is therefore necessary to provide small-scale and low-cost solutions that do not require advanced technology and abundant energy resources to produce fresh water. The present works focus on solar desalination, which as the name suggest relies on solar radiation. The device known as solar still counts on this sustainable energy source to produce freshwater. An alternative thermal modeling approach, which compromises a coupled energy balance for each component individually of the solar still, is provided, so that its accuracy is increased for different designs, locations and ambient conditions. The model is able to capture the physical evolution of the solar still, following the water temperature quite well, and predicts the water yield with a maximum deviation around 6% for the evaluated experiments. Moreover, in a selected experiment from the literature, a parametric analysis is performed to further understand how to improve the water yield. The parameters that must be optimized are water depth, walls height, scaling of the structure, insulation, incident solar radiation and basin-glass temperature difference. Finally, based on the parametric study and on the identified improvement solutions from the literature, feasible real options are analysed, such as modification of the solar still design (up to 19% and 70% on a summer and winter day, respectively), external/internal reflectors addition (up to 21%/7% and 73%/79% on a summer and winter day, respectively) and glass cooling cover (up to 29% for large water quantities, low/none effect on smaller ones). Moreover, preliminary studies on evaporation and condensation separation (up to 80%); as well as use of a porous medium fan inside (up to 22%), use of a porous medium (up to 10%), better insulation (up to, are presented, modeled and their impact is evaluated.
Keywords: Solar desalination, Solar still, Thermal modelling, Water yield enhancement

1. Introduction

Water is one of the most vital and yet finite resource in the world. Only 3% of all water in the world is fresh water and only about a third of it is easily accessible. In recent years, growing water consumption together with increasing pollution, global warming and poor management of water resources have led to increased water stress worldwide. This natural resource is not evenly distributed and many regions still lack adequate access to usable water sources. Desalination is seen as a viable solution, however conventional desalination techniques for obtaining fresh water, such as reverse osmosis and modern thermal processes, consume large amounts of energy, technological resources and infrastructure that are lacking in less developed countries. Since the use of these technologies is not feasible, solutions must be offered on a small scale and at low cost. Solar desalination is an alternative approach to the production of fresh water that is usually associated to a device known as solar still. The solar still only depends on the globally available solar radiation to operate, adding to the fact that it is easy to build and simple to maintain. Despite all these advantages, the conventional solar still produces about 2-3 liters per square meter [1], which is not enough to satisfy the end user.

2. Solar Still

The simplest design of the solar still is the single basin and slope, schematically represented in Fig. 1. Structure wise, the device basin and walls are usually made of materials with low specific heat capacity and high thermal conductivity, such as aluminum or iron, and painted black to maximize absorption of incident radiation. The basin is continuously fed and covered with seawater. On the upper side, a sloped glass cover with high transmissivity is installed to allow the maximum radia-

tion to reach the inside. At the bottom of the inclined glass, there is a pipe to collect the condensation water. The solar still is sealed to prevent air exchange with the environment and well insulated, e.g. with glass wool or sawdust, to prevent heat loss.

2.1. Experimental Performance Enhancement

Numerous experimental studies investigating various parameters have been carried out to increase the water yield, thus it is important to analyze and understand some of the studies.

To increase the solar radiation Lei Muet al. [2] used a Fresnel lens and they were able to increase the water yield by 467.4% , however, the lens had to be constantly adjusted to the suns's position. Omara et al. [3, 4] investigated the advantage of using reflectors on the back inner wall of a stepped solar still with an improvement of 75%, and with both inner and exterior reflectors resulting in an improvement of 125% compared to the conventional solar still. Tanaka [5] investigated the advantage of using a conventional solar still with both the internal and external reflectors improving the yield by 70%.

Countless studies have been conducted to prove that the optimal tilt angle of the cover must be equal to the latitude of the sun's position to achieve maximum production all year round.

The influence of water depth is also frequently found in the literature, and it is concluded that decreasing water depth increases the performance of the solar stills.

Many designs were tested, from single slope glass cover to double slope, pyramid-shaped and hemispherical glass cover [6]. There is a consensus in the literature that increasing the glass cover area promotes more condensation [7]. Another effective design approach is to use a stepped basin solar still.

Researchers have investigated techniques that allow water production to continue after sunset. For examples, Tabrizi et al.[8] investigated the effect of a sand reservoir under the basin.

The promotion of convection within the enclosure with a small fan at low speed, as performed by Kianifar et al. [9], can increase mass transfer and consequently condensation.

Porous materials have been increasingly used because of their advantage of combining the properties of water and porous medium. Murugavel et al. [10] used different wick materials which resulted in water yield improvement. Bilal et al. [11] covered the basin with pumice stones, however, it deteriorated the still performance.

Another option is to reduce the glass temperature to dissipate the condensation heat. The goal is to increase the basin-glass temperature difference, so that mass transfer and thus condensation augments. Cooling the glass cover maybe done by using a fan or a water film. For example, Badran [12] installed a sprinkler above the glass cover, which increased the water yield by 20%.

2.2. Thermal Model

Predicting with precision and simplicity the water production of solar stills with different designs and at different locations is an important task that avoids time-consuming experimental work. Thermal models are made of energy balances of the solar still components. The thermal models seen in the literature use the same general energy equations for the basin, water and glass and differ only in the correlations for convective and evaporative heat transfer between water and glass. The most popular thermal model is the Dunkle's [13] model which is a simple model with various simplifications, which is intended for a double slope solar still. However, it is generally observed that it is used for all structures and sometimes does not fall under the limitations of the model. Some details, such as solar radiation, wall losses, shadows, are not given in the model, and it is common to see different refinements.

The present research work aims to present a thermal model that differs from others since it acknowledges energy balances for all solar still components and the air within, thus creating a simulation that better represents reality. In addition, a parametric study will be carried out to understand how water production can be improved. Finally, based on the parametric study and the literature, real-world approaches to be implemented are evaluated.

3. Alternative thermal model approach

The results are obtained by solving of the energy balance equations for the basin, seawater, walls and glass cover.

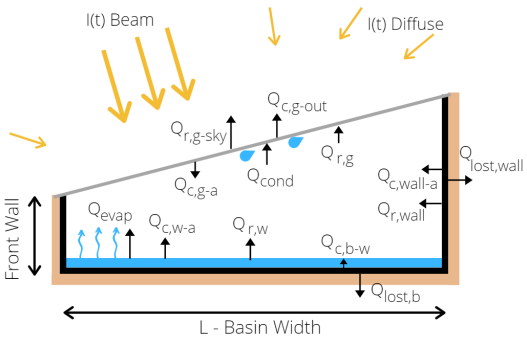

Figure 1: Schematic view of solar still heat transfer processes. The remaining walls have similar heat exchanges as the one represented. Legend: Black - basin/wall, Blue - seawater, Brown - insulation

Energy balance for the glass:

$$(mc_p)_g \frac{\partial T_g}{\partial t} = Q_{sun,g} + Q_{cond} + Q_{r,g} + Q_{c,a-g} - Q_{r,g-sky} - Q_{c,g-out} \quad (1)$$

The input energy results from the absorbed solar radiation ($Q_{sun,g}$), the convection heat transfer between air and glass ($Q_{c,a-g}$), the latent heat of the condensed water (Q_{cond}) and the radiation heat transfer between glass and the remaining surfaces ($Q_{r,g}$). The absorbed solar radiation is divided into direct (I_{dr}), and diffuse radiation (I_{dif}). The absorption coefficient of each surface is given by α and the correspondent surface subscript.

$$Q_{sun,g} = \alpha_g A_g (I_{dr,g} + I_{dif,g}) \quad (2)$$

$$Q_{c,a-g} = h_{c,a-g} A_g (T_a - T_g) \quad (3)$$

$$Q_{cond} = \dot{m}_{cond} \triangle H_{H_2O} \quad (4)$$

The glass exchanges heat by radiation with water and walls. The summatory in Eq. 7 accounts for the radiation from front, back, and lateral walls. The respective view factor, F_{1-2}, must be computed for each radiation heat exchange (subscript $1-2$ represent the surfaces that interact).

$$Q_{r,g} = Q_{r,w-g} + Q_{r,walls-g} \quad (5)$$

$$Q_{r,w-g} = h_{r,w-g} A_w (T_w - T_g) F_{w-g} \quad (6)$$

$$Q_{r,walls-g} = \sum h_{r,wall-g} A_{wall} (T_{wall} - T_g) F_{wall-g} \quad (7)$$

The glass loses heat in the form of radiation to the atmosphere and because of the convective heat transfer caused by wind,

$$Q_{r,g-sky} = h_{r,g-sky} A_g (T_g - T_{sky}) \quad (8)$$

$$Q_{c,g-out} = h_{c,g-out} A_g (T_g - T_{out}) \quad (9)$$

Energy balance for the basin:

$$(mc_p)_b \frac{\partial T_b}{\partial t} = Q_{sun,b} - Q_{c,b-w} - Q_{lost,b} \quad (10)$$

The basin gains heat by absorbing incident radiation, $Q_{sun,b}$, and loses heat to the water above it by convection, $Q_{c,b-w}$, and to the exterior, $Q_{lost,b}$.

$$Q_{sun,b} = I_{dr,b} (\tau_g)_{dr} \tau_w \alpha_b A_{exp,b} + I_{dif} (\tau_g)_{dif} \tau_w \alpha_b A_b \quad (11)$$

$$Q_{lost,b} = A_b U_b (T_b - T_{out}) \quad (12)$$

Energy balance for the seawater:

$$(mc_p)_w \frac{\partial T_w}{\partial t} = Q_{sun,w} - Q_{evap} - Q_{r,w} - Q_{c,w-a} + Q_{c,b-w} - \dot{m}_{evap} (T_w - T_{out}) c_{pw} \quad (13)$$

The water is heated due to the incident solar radiation, $Q_{sun,w}$, and convection heat from the basin, $Q_{c,b-w}$.

$$Q_{sun,w} = I_{dr,w} (\tau_g)_{dr} \alpha_w A_{exp,w} + I_{dif,w} (\tau_g)_{dif} \alpha_w A_w \quad (14)$$

$$Q_{c,b-w} = A_w h_{c,b-w} (T_b - T_w) \quad (15)$$

It loses heat by giving away energy for water evaporation, Q_{evap}, convection, $Q_{c,w-a}$, and radiation, $Q_{r,w}$.

$$Q_{evap} = \dot{m}_{evap} \triangle H_{H_2O} \quad (16)$$

$$Q_{c,w-a} = A_b h_{c,w-a} (T_w - T_a) \quad (17)$$

$$Q_{r,w} = Q_{r,w-g} + Q_{r,w-walls} \quad (18)$$

$$Q_{r,w-walls} = \sum h_{r,w-wall} A_w (T_w - T_{wall}) F_{w-wall} \quad (19)$$

Energy balance for the wall:

$$(mc_p)_{wall} \frac{\partial T_{wall}}{\partial t} = Q_{sun,wall} + Q_{r,w-wall} - Q_{r,wall-g} - Q_{c,a-wall} - Q_{lost,wall} \quad (20)$$

The walls absorb incident solar radiation, $Q_{sun,wall}$, and lose heat by convection due to interaction with the enclosure's air. They also lose heat by radiation exchange with other surfaces, and to the exterior by conduction.

$$Q_{sun,wall} = I_{dr,wall} (\tau_g)_{dr} \alpha_{wall} A_{exp,wall} + I_{dif_{wall}} (\tau_g)_{dif} \alpha_{wall} A_{wall} \quad (21)$$

$$Q_{lost,wall} = A_{wall} U_{wall} (T_{wall} - T_{out}) \quad (22)$$

Energy balance for the air:

$$(mc_p)_a \frac{\partial T_a}{\partial t} = Q_{c,w-a} + Q_{c,wall-a} - Q_{c,a-g} \quad (23)$$

The air's heat gain or loss is due to the heat transfer convection mechanisms when it interacts with water, walls, and glass.

3.1. Incident solar radiation

3.1.1 Beam and diffuse radiation

Commonly from the available solar radiation data, it is possible to get the global solar radiation on a horizontal surface. In a simplified approach, it can be assumed that this global irradiance is the sum the direct/beam radiation,I_{dr}, and the diffuse,I_{dif}, thus they must be split. The I_{dr} only reach non-shaded areas and I_{dif} absorbed by each component depends on the view factor. Moreover, based on the literature, different transmissivities and absorption estimates are given for the materials depending on the type of radiation component.

One of the widely used correlations that is used to compute I_{dif}, is the Orgill and Hollands correlation [14],

$$\frac{I_{dif}}{I_G} = \begin{cases} 1 - 0.249k_t & \text{for } 0 \leq k_t \leq 0.35 \\ 1.5571.84k_t & \text{for } 0.35<k_t<0.75 \\ 0.177 & \text{for } k_t>0.75 \end{cases} \quad (24)$$

The clearness sky index, k_t, differs for each location and season as well as along the day. In the literature, the available information is relative to the average monthly sky clearness index for some locations, which is going to be used to calculate radiation values. By computing the I_{dif}, consequently it is possible to obtain I_{dr}.

The solar still glass is inclined with the respective angle, β_g, thus it will not view the entire sky. Diffuse radiation must be corrected with the appropriate view factor

$$I_{dif,g} = I_{dif}\left(\frac{1+\cos\beta_g}{2}\right) \quad (25)$$

The diffuse radiation absorbed by basin and walls depends on the view factor to the glass. As an example, for the walls,

$$I_{dif,wall} = I_{dif,g}\left(\frac{1+\cos\beta_{wall}}{2}\right)F_{wall-g} \quad (26)$$

The absorbed beam radiation , I_{dr}, is calculated according to the position of the sun and the surface inclination.The geometric factor, R, is the ratio of beam radiation on the inclined surface to that on a horizontal surface.

$$R = \frac{I_{dr,tilted}}{I_{dr,horizontal}} = \frac{\cos\theta}{\cos\theta_z} \quad (27)$$

These equation carry new variables, such as, θ, which is the angle of incident radiation on a surface, and, θ_z, which is the zenith angle. It is possible to obtain them, by using the following correlations,

$$\begin{aligned}\cos\theta = {} & \sin\delta\sin\phi\cos\beta - \sin\delta\cos\phi\sin\beta\cos\gamma \\ & + \cos\delta\cos\phi\cos\beta\cos\omega + \cos\delta\sin\phi\sin\beta \\ & \cos\gamma\cos\omega + \cos\delta\sin\beta\sin\gamma\sin\omega\end{aligned} \quad (28)$$

$$\cos\theta_z = \cos\delta\cos\phi\cos\omega + \sin\phi\sin\delta \quad (29)$$

where, it is used the surface azimuth angle, γ, the hour angle, ω, and the sun declination angle, δ. It is necessary to compute ω and δ,

$$\omega = 15(t_{solar} - 12) \quad (30)$$

$$\delta = 23.45\sin\left(360(284+n)/365\right) \quad (31)$$

The term t_{solar} corresponds to solar local time, and n to the day number. To compute t_{solar},

$$t_{solar} = t + \frac{4(\lambda - LSTM) + EoT}{60} \quad (32)$$

where, t represents the local time of the time step, λ the longitude, $LSTM$ is the Local Standard Time Meridian, and EoT is the equation of time to refine the solar hour. All these values can be computed with,

$$LSTM = 15 \times \Delta T_{UTC} \quad (33)$$

$$EoT = 9.87\sin(2B) - 7.53\cos(B) - 1.5\sin B \quad (34)$$

$$B = \frac{360}{365}(n-81) \quad (35)$$

where, ΔT_{UTC} is the difference of the Local Time from Universal Coordinated Time in hours. If there is daylight saving time , it should be taken 1h from t.

3.1.2 Material radiative properties

Detailed attention is given to the calculation of the radiation properties of glass and basin/wall, more precisely the transmissivity and absorption, respectively. Two approaches were studied, the first with constant radiative properties, and the second dependent on the solar radiation angle of incidence. The second approach will be described since it is considered the most suitable.

Looking at the glass properties, Tanaka [15] gives a relation between glass transmissivity and beam radiation incident angle (θ, given in Eq. 28) .

$$\begin{aligned}\tau_g(\theta) = {} & 2.642\cos\theta - 2.163\cos^2\theta - 0.320\cos^3\theta \\ & + 0.719\cos^4\theta \qquad (glass\ 3mm\ thick)\end{aligned} \quad (36)$$

Moreover, Tanaka also gives the transmissivity to diffuse radiation dependent on the glass cover angle.

$$(\tau_g)_{df} = -2.03\times10^{-5}\times\beta^2 - 2.05\times10^{-3}\times\beta + 0.667 \quad (37)$$

For the glass radiation absorption, it was assumed $\alpha_g = 6\%$.

The water radiative properties were chosen taking into account that water depth normally is chosen to be as small as possible. It was assumed a $\tau_w = 93\%$ and $\alpha_w = 5\%$ The values chosen are commonly seen in the literature.

For the basin, the most important parameter is α_b. The ratio of absorption to normal absorption, is given by,

$$\begin{aligned}\frac{\alpha}{(\alpha)_n} &= 1 - 1.5879 \times 10^{-3}\theta + 2.7314 \times 10^{-4}\theta^2 \\ &- 2.3026 \times 10^{-5}\theta^3 + 9.0244 \times 10^{-7}\theta^4 \\ &- 1.8 \times 10^{-8}\theta^5 + 1.7734 \times 10^{-10}\theta^6 \\ &- 6.9937 \times 10^{-13}\theta^7\end{aligned} \tag{38}$$

For the absorption of diffuse radiation by basin (horizontal surface) and walls (vertical surfaces), the effective incidence angle will be close to 60 , corresponding to 90% radiation absorption [14].

3.1.3 Shadows model

Let us now look at the simplified shadow model. Instead of computing in detail the dimensions of the shadow, it is computed an average shadow height. First it is necessary to compute solar altitude, α_{sun}, and the azimuth , ϕ, for each time step to get an approximate shadow length.

$$\sin \alpha_{sun} = \sin \Phi \sin \delta + \cos \Phi \cos \delta \cos h \tag{39}$$

$$\sin \phi = \frac{-\sin h \cos \delta}{\sin (90 - \alpha_{sun})} \tag{40}$$

It is possible to get e and g, using the front an back wall height, respectively.

$$e/g = \frac{H_{wall,front/back}}{\tan(\alpha_{sun})} \sin(90 - \phi) \tag{41}$$

By performing the following equation, the values f and h, can be computed, using the front an back wall height, respectively,

$$f/h = \frac{H_{wall,front/back}}{\tan(\alpha_{sun})} \sin(\phi) \tag{42}$$

For the case represented in Fig. 2, the area imposed by the front wall and lateral wall are respectively computed as,

$$A_{Shaded,Front} = f \times C \tag{43}$$

$$A_{Shaded,Lateral} = \frac{e+g}{2} \times C \tag{44}$$

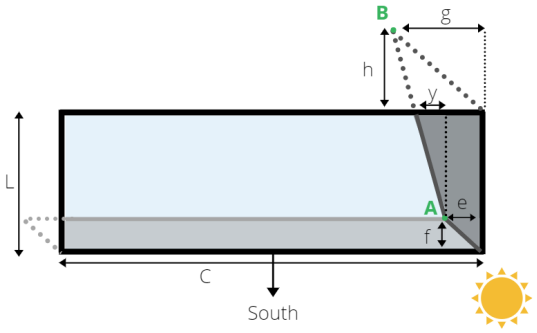

Figure 2: Solar still covered by front and lateral wall shadow, for $|\phi| < 90$

For the case represented in Fig. 3, the area imposed by the back wall and lateral wall are respectively computed as,

$$A_{Shaded,Front} = h \times C \tag{45}$$

$$A_{Shaded,Lateral} = \frac{e+g}{2} \times C \tag{46}$$

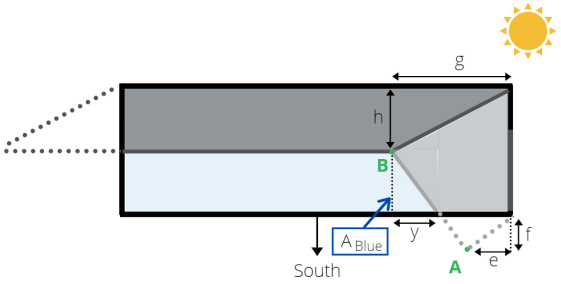

Figure 3: Solar still covered by back and lateral wall shadow, for $|\phi| > 90$

For both simplified and detailed shadow model, the area exposed to incident beam radiation will be,

$$A_{Exp,b} = A_b - (A_{Shaded,Back/Front} + A_{Shaded,Lateral}) \tag{47}$$

The simplified shadow model, as the name suggests is quite simple and there is some overlap when performing the sum of the shadows. Nonetheless, study was conducted to check how both shadow models affect the water yield and it was found that the deviation is about 3%.

To model shadow on the walls a simplified approach was chosen and the following considerations were taken into account:

1. All walls shaded, when the solar azimuth angle is greater than 90and smaller than -90, since the sun is behind the still and generally with low solar altitude.

2. Front and one side wall shade (right, if $\phi > 0$ or left, $\phi < 0$), when the solar azimuth angle is between -90and 90. Shadow on back wall due to side walls.

The shadow on the back wall when $-90 < \phi < 90$, is computed by using and average shadow height of the lateral walls, and the height of the back wall ,

$$A_{Shaded,Back} = \frac{e+g}{2} \times H_{wall,Back} \quad (48)$$

$$A_{Exp,Back} = A_{wall,Back} - A_{Shaded,Back} \quad (49)$$

For the shaded area on the lateral walls, when $-90 < \phi < 90$, an approximate exposed area is computed,

$$A_{Shaded,Lateral} = e \times H_{wall,Front} \quad (50)$$

$$A_{exp,wall_{Lateral}} = A_{wall_{Lateral}} - A_{Shaded,Lateral} \quad (51)$$

3.2. Heat transfer mechanisms

The proposed approach differs from other thermal models because it includes the analysis of walls and air. The air is modeled fairly simple being it considered a homogeneous body, meaning that water content and temperature are assumed evenly distributed.

3.2.1 Convection

It was decided to use free convection correlations for each surface, even though the processes occur inside the solar still.

The following Nusselt numbers correlations are taken from the same literature reference [16]. To compute the heat transfer coefficient for the walls, $h_{c,wall-a}$, the following correlation is used,

$$Nu_L = \left(0.825 + \frac{0.387 Ra_L^{1/6}}{(1 + (0.492/Pr)^{9/16})^{8/27}} \right) \quad (52)$$

Assuming the basin temperature to be higher than water, and water at a higher temperature than air, it is possible to compute heat transfer coefficient between basin and water, $h_{c,b-w}$, and water and air, $h_{c,w-a}$, with Eq. 53 and 54, respectively.

$$Nu_L = 0.54 Ra_L^{1/4} \qquad (10^4 < Ra_L < 10^7) \quad (53)$$

$$Nu_L = 0.15 Ra_L^{1/3} \qquad (10^7 < Ra_L < 10^{11}) \quad (54)$$

The glass is a downward inclined cold surface, and for these cases, there is less agreement in the literature.There are references for the upward inclined hot surface, being one of the main referenced studies from Fuji [17] and Vliet [18] . The correlation which showed better performance was the one from Fuji, in Eq. 55. Furthermore, a similarity relationship has been assumed between convection on upward inclined hot surfaces and downward inclined cold surfaces.

$$Nu_L = 0.13((GrPr)^{1/3} - (Ra_c)^{1/3}) + 0.56(Gr_c Pr \cos\beta_g)^{1/4} \quad (55)$$

where,

$$Ra_c = 0.3 \times 10^7 \exp(0.18\beta_g) \qquad [18] \quad (56)$$

3.2.2 Radiation

Radiation heat transfer takes place within the solar still between the water mass with the glass cover and the walls and between the walls and the glass cover. Since all components are modeled, it is important to determine the appropriate view factors (F_{1-2}) to obtain an accurate simulation.

To calculate the radiant heat transfer coefficient is used Eq. 57 , where the subscript indices 1 and 2 represent the considered surfaces.

$$h_{r,1-2} = \epsilon\sigma(T_1^2 + T_2^2)(T_1 + T_2) \quad (57)$$

It is important to stress the necessity to choose the correct view factors between surfaces, so that the correct heat exchanged by radiation is computed.

$$Q_{r,1-2} = h_{r,1-2} A_1 (T_1 - T_2) F_{1-2} \quad (58)$$

3.2.3 Losses

Radiation lost by the glass to the environment is given by the known radiation exchange formula in Eq. 57, more specifically,

$$h_{r,g-sky} = \epsilon\sigma(T_g^2 + T_{sky}^2)(T_g + T_{sky}) \quad (59)$$

The sky temperature, which accounts for a nonuniform temperature of the atmosphere and the radiation exchange only in certain wavelength ranges [1, 14], can be calculated with the following equation,

$$T_{sky} = 0.0552 T_{out}^{1.5} \quad (60)$$

One of the most used correlation for external losses because of the wind (v is the wind velocity), is given by Watmuff and Charters [19],

$$h_{c,g-out} = 2.8 + 3v \qquad (0 < v < 7m/s) \quad (61)$$

Performing an analogy between heat transfer and electric current, basin and walls lose heat due to thermal conduction through the insulating material (Li is the insulation thickness and K_i it's thermal conductivity) and external convection. The overall heat transfer coefficient can be computed as follows,

$$U = \left(\frac{Li}{Ki} + \frac{1}{h_{c,g-out}} \right)^{-1} \quad (62)$$

3.2.4 Evaporation/Condensation

It is assumed that the water evaporating from the basin is immediately renewed and thus the seawater mass on the basin remains constant. It is also assumed that the water condensing on the glass is collected immediately.

Following Örvös et al. [20] work ,

$$\dot{m}_{evap} = A\frac{h_{c,w-a}}{(cp)_a}(w_w - w_a) \tag{63}$$

where, w is given as,

$$w = \frac{M_{H_2O}}{M_a}\frac{\varphi p_{v,sat}}{P - p_{v,sat}} \tag{64}$$

and,

$$p_{v,sat} = \exp\left(\frac{25.317 - 5144}{T}\right) \tag{65}$$

Condensation is done similarly to evaporation, being the only difference that the mass transfer now is from the moist warm air to the cold glass.

$$\dot{m}_{cond} = \frac{h_{c,a-g}}{(cp)_a}(w_a - w_g) \tag{66}$$

At the end of each time step, it is needed to compute φ, so that the evaporated and condensed water from the following time step can be calculated. It is necessary to calculate the sum of the water existing in the air, $m_{v,a_{t-1}}$, with the difference between evaporated and condensed water in that time step, $(\dot{m}_{evap} - \dot{m}_{cond})\Delta t$.

$$m_{v,a} = m_{v,a_{t-1}} + (\dot{m}_{evap} - \dot{m}_{cond})\Delta t \tag{67}$$

The vapour pressure is given by,

$$p_{v,a} = \frac{m_{v,a}RT_a}{M_{H_2O}V} \tag{68}$$

and finally,

$$\varphi = \frac{p_{v,a}}{p_{v,sat}} \tag{69}$$

3.3. Implementation of the thermal model

For each time step, the model calculates the temperatures of basin, walls, air, water and glass as well as the water yield, as described in section 3. The temperatures and the cumulative water are computed and plotted, for the experimental work carried out by Kabeel et al. [21]. The experimental data can be compared (dashed line) with the theoretical estimate (thick line), shown in Figs. 4 and 5. The simulation follows the physical evolution of the different evaluated parameters with accuracy.

Larger discrepancies are found between the estimated and the experimental glass temperature. It is not known if the thermocouple is located on the outter or inner side of the glass, which influences the temperature measured. Nevertheless, the water temperature, which is considered to be the most reliable measured temperature, can be well followed, presenting small deviations.

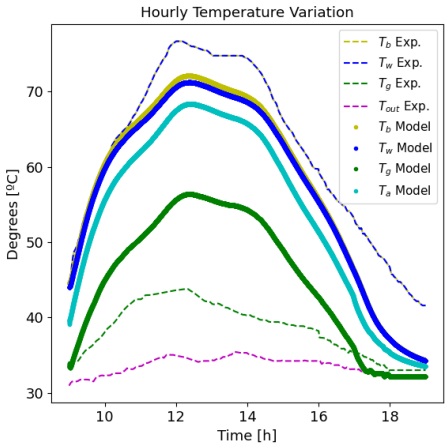

Figure 4: Hourly temperature variation for the proposed model, as well as the data from the experiment carried out by Kabeel et al. [21]

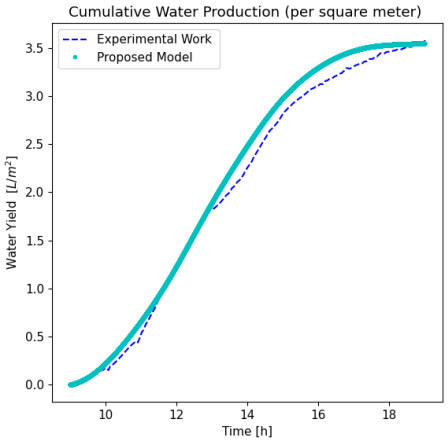

Figure 5: Cumulative water yield for the proposed model, as well as the data from the experiment carried out by Kabeel et al. [21]

4. Parametric study

To achieve the maximum water yield, a parametric study is carried out to characterize the variables that can optimize the solar still. Some subsections provide the deviation of the water yield for a representative winter day.

4.1. Scaling

Since the glass angle should correspond to the latitude of the location so that the maximum solar radiation reaches the basin all year round, the most

appropriate scaling option is to increase the length (C) of the solar still. If the width (L) were to be increased, the cover glass would have to have a larger height, which is not a practical design solution. Walls and glass height remain the same. Fig. 6 shows that shorter lengths mean a reduction in water production as the area exposed to radiation decreases. On a summer day, increasing the solar still length has a smaller effect than in the winter, because the exposed area is already close to the maximum.

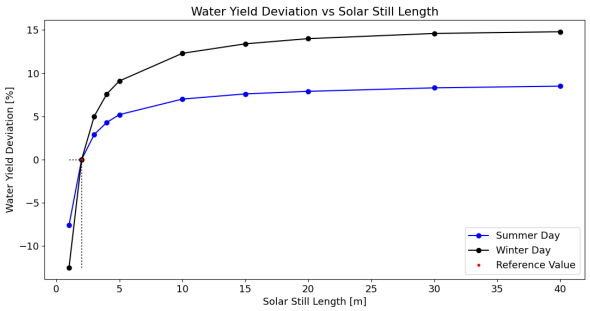

Figure 6: Water yield deviation as function of scaling the solar still, more specifically by changing the still length.

Larger lenghts have an increasingly smaller impact on water production because the ratio between the exposed area and the shaded area does not vary significantly.

4.2. Water depth

One of the most studied parameters in the literature is water depth, which is related to the amount of water mass inside the still. Less water mass and thus less thermal inertia mean that the water temperature can be further increased, enhancing evaporation.

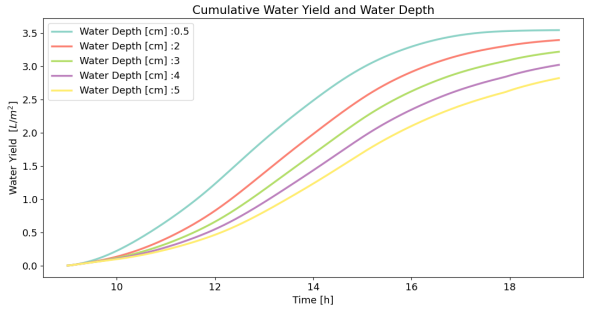

Figure 7: Sensitive analysis to water yield as function of water depth

4.3. Insulation

The worse the insulation, the less effective the performance of the solar still is. The ideal case would be to have the solar still perfectly insulated, however adding a large amount of insulation is not the solution, as the improvements tend to be small above a certain value. Moreover, the more insulation is used, the more expensive an heavy the still becomes.

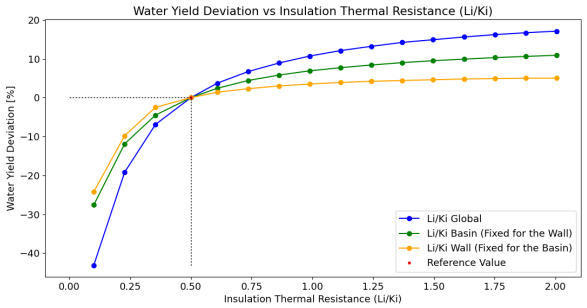

Figure 8: Sensitive analysis to water yield as function of L_i/K_i

It is possible to infer that both basin and wall insulation is important for the still performance. If it is not possible to increase global insulation, it is preferred to add more insulation to the basin than to the walls.

4.4. Condensation

One of the problems of the solar still is that evaporation and condensation occur in the same physical space, consequently, condensation will act as bottleneck of water production. Moreover, heat and mass transfer processes are due to the natural convection promoted by water-glass temperature difference. Increasing this temperature difference enhances the convection inside the still and thus augment the water yield. In this study, it was assumed that the temperature of the walls is equal to the air temperature. By varying the glass temperature for a fixed basin temperature, it is possible to confirm the enhancement of water production for increasing basin-glass temperature difference, as shown in Fig. 9.

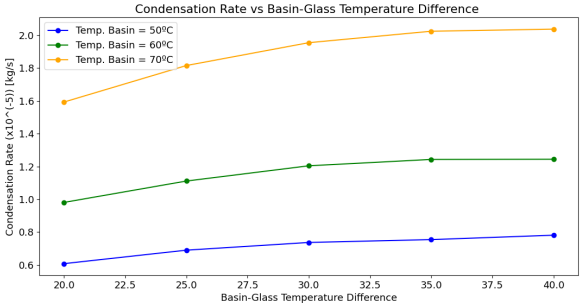

Figure 9: Sensitive analysis of condensation rate as function of $\Delta(T_b - T_g)$

5. Performance Enhancement

In this section, the real approaches with the greatest impact are presented.

5.1. Solar still structure

A reduction in wall height directly reduces heat loss, as less wall surface comes into contact with the outside. In addition to this benefit, smaller walls mean less shading and therefore more incident solar radiation. To perform this study, the height of the front wall (lowest wall of the solar still) is attributed and from this value the dimensions of the other walls are calculated.

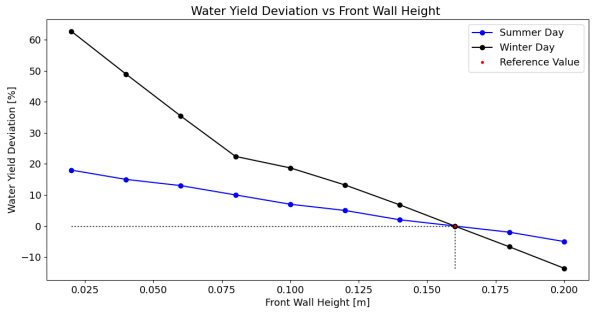

Figure 10: Water yield deviation as a function of low wall height, for a representative summer and winter day. This height influences the computing of the remaining walls and consequently the associated shadows.

5.2. Use of Reflectors

Using internal and/or external reflectors/mirrors increases the solar radiation on the basin. Tanaka examined this topic in more detail, theoretically and experimentally, thus the reasoning has similarities with his work.

5.2.1 External reflector

The external reflector is easy to install , and it can be tilted according to the season to increasing incident reflect solar radiation. Water yield improvement depends on the dimensions of the reflector. In this study, it was assumed that it has the same dimensions as the back wall. Figure 11 presents an analysis for a summer and a winter day to observe the effect of adding the external reflector.

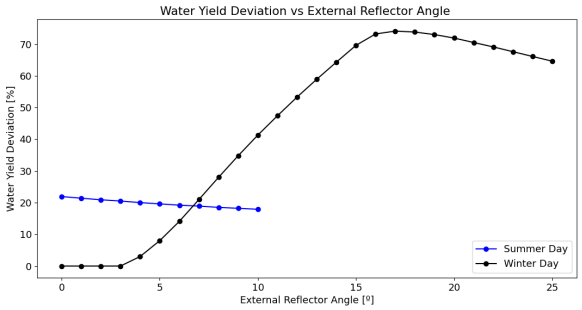

Figure 11: Water yield deviation as a function of external reflector angle, for a representative summer and winter day. Mirror is tilted until the angle does not allow solar radiation reflected to the back wall.

In the summer, mounting the reflector, automatically increases the water yield, however, increasing the reflector angle does not bring any benefits. In winter, the sun is at lower altitude, and because the external reflector is mounted above the back wall, no reflected solar radiation reaches the basin unless the reflector is tilted. The external reflector must be tilted according to the season.

5.3. Reducing glass temperature

Reducing glass temperature by using a fan or a water film only revealed improvement in yield if large quantities of water were in the solar still. This study analyses the effect of increasing wind speeds on the glass cover. Note that Fig. 12 may give the false impression that greater water production is achieved for the greater water depth. This is not the case, the greatest percentage improvement in water yield will be in the 5 cm water depth, but when comparing the yield values themselves, it can be seen that 0.5cm water depth is preferred, as shown in Table 1.

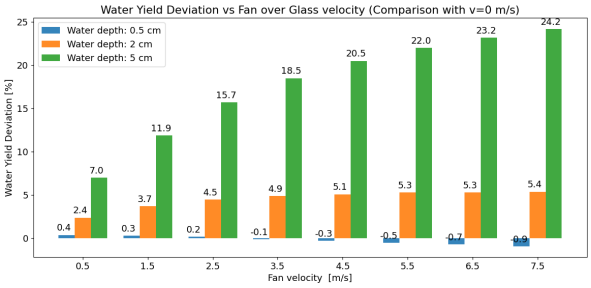

Figure 12: Water yield deviation for three water depths, as function of the glass cover wind velocity. Results are compared to no wind velocity on the glass cover.

Water Depth	**v = 0 m/s**	v = 7.5 m/s	Deviation
0.5 cm	**3.55**	3.53	-0.9%
2 cm	**3.24**	3.42	+5.4%
5 cm	**2.34**	2.9	+24.2%

Table 1: Water yield (L/m^2) and water yield deviation for different water depths and glass wind velocities. In bold a reference case with no wind velocity on the glass cover.

5.4. Separate evaporation and condensation

Separating condensation and evaporation enables greater evaporation of the basin water, as it is no longer restricted by condensation. The theoretical analysis is similar to Hammadi [22], however, additional studies are done. Of the many studies done, it was inferred that for this technique to be advantageous, the evaporator has to be long, and inlet mass air flow must be small, with high velocity and φ. Moreover, the lower the temperature of the cold reservoir to condense water vapour, the better.

In Fig. 13 it is possible to infer that water production of this technique can exceed the conventional still water yield. The study was also investigated for a air supply with $\varphi = 30\%$, however, it did not exceed the conventional solar still productivity. Moreover, with larger inlet area, it also could not exceed the conventional solar still.

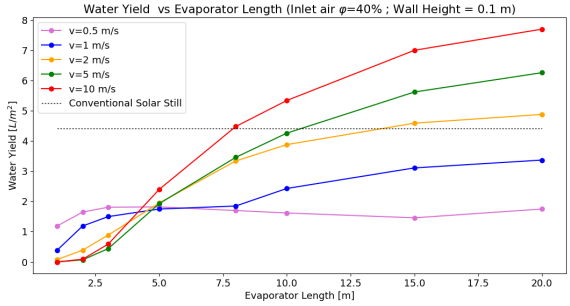

Figure 13: Water yield as a function of evaporator length, for different velocities. Intake air with 40% relative humidity, and wall height of 0.1m . Conventional solar still yield: 4.42 L/m^2

6. Conclusions

This work presented a alternative thermal model capable of predicting the performance of the solar still. The provided model is more intuitive to understand since all the thermodynamic processes are modeled in detail, which enables a better parameter optimization. Moreover, real approaches to enhance water yield were evaluated. It is important to examine the different options before building the solar still.

References

[1] G.N. Tiwari and L. Sahota. *Advanced Solar-DistillationSystems*, pages 21–36. Springer, 2017.

[2] L.Mu, X.Xub, T.William, C. Debrou, R. Gomez, Y. Park, H. Wang, K. Kota, P. Xub, and S. Kuravia. Enhancing the performance of a single-basin single-slope solar still by using fresnel lens: Experimental study. *Journal of Cleaner Production*, 239, December 2019. doi:10.1016/j.jclepro.2019.118094.

[3] Z.M.Omara, A.E.Kabeel, and M.M.Younesa. Enhancing the stepped solar still performance using internal reflectors. *Desalination*, 314, April 2013. doi:10.1016/j.desal.2013.01.007.

[4] Z.M.Omara, A.E. Kabeel, and M.M. Younes. Enhancing the stepped solar still performance using internal and external reflectors. *Energy Conversion and Management*, 78:876–881, 2014. doi:10.1016/j.enconman.2013.07.092.

[5] H. Tanaka. Experimental study of a basin type solar still with internal and external reflectors in winter. *Desalination*, 249:130–134, 2009. doi:10.1016/j.desal.2009.02.057.

[6] P. Vishwanath, K. Om K. Anil, P. Ajay, and K. Kaviti. Solar stills system design: A review. *Renewable and Sustainable Energy Reviews*, 51:153–181, June 2015. doi:10.1016/j.rser.2015.04.103.

[7] Z.M.Omaraa, A.Abdullah, A.E.Kabeelb, and F.A.Essaa. The cooling techniques of the solar stills' glass covers – a review. *Renewable and Sustainable Energy Reviews*, 78:176–193, October 2017. doi:10.1016/j.rser.2017.04.085.

[8] F.F. Tabrizi and A.Z.Sharak. Experimental study of an integrated basin solar still with a sandy heat reservoir. *Desalination*, 253:195–199, April 2010. doi:10.1016/j.desal.2009.10.003.

[9] O. Mahian and A. Kianifar. Mathematical modelling and experimental study of a solar distillation system. *Journal of Mechanical Engineering Science*, 225:1203–1212, April 2011. doi:10.1177/2041298310392648.

[10] K.K. Murugavel and K.Sritharb. Performance study on basin type double slope solar still with different wick materials and minimum mass of water. *Renewable Energy*, 36:612–620, February 2011. doi:10.1016/j.renene.2010.08.009.

[11] A. Bilal, B. Jamil, N. Ul Haque, and Md Azeem Ansari. Investigating the effect of pumice stones sensible heat storage on the performance of a solar still. *Groundwater for Sustainable Development*, 9, October 2019. doi:10.1016/j.gsd.2019.100228.

[12] O.O. Badran. Experimental study of the enhancement parameters on a single slope solar still productivity. *Desalination*, 209:136–143, April 2007. doi:10.1016/j.desal.2007.04.022.

[13] R.V. Dunkle. Solar water distillation, the roof type still and multiple effect diffusion still. Proceedings of the International Heat Transfer Conference, Part V—International Developments in Heat Transfer, 1961. pp. 895–902.

[14] J.A. Duffie and W. A. Beckman. *Solar Engineering of Thermal Processes*. Wiley.

[15] H. Tanaka and Y.Nakatake. Theoretical analysis of a basin type solar still with internal and external reflectors. *Desalination*, 197:205–216, 2006. doi:10.1016/j.desal.2006.01.017.

[16] T. Bergman, F. Incropera, D DeWitt, and A. Lavine. *Fundamentals of Heat and Mass Transferr*, volume 6, pages 560–618. John Wiley Sons, 2007.

[17] T. Fuji and H. Imura. Natural-convection heat transfer from a plate with arbitrary inclination. *Journal of Heat and Mass Transfer*, 15:755–764, 1979. doi:10.1016/0017-9310(72)90118-4.

[18] G. Vliet. Natural convection local heat transfer on constant-heat-flux inclined surfaces. *Journal of Heat Transfer*, 91:511–516, 1969. doi:10.1115/1.3580235.

[19] J Watmuff, W Charters, and D. Proctor. Solar and wind induced external coefficients solar collectors. Technical report, Revue International d'Helio- technique,, 1977.

[20] M. Örvös, V. Szabó, and T. Poós. Rate of evaporation from the free surface of a heated liquid. *Journal of Applied Mechanics and Technical Physics*, 57:1108—-1117, 2016. doi:10.1134/S0021894418010248.

[21] A.E.Kabeel, A.Khalil, M.Omara, and M.M.Younes. Theoretical and experimental parametric study of modified stepped solar still. *Desalination*, 289:12—-20, 2012. doi:10.1016/j.desal.2011.12.023.

[22] S. H.Hammadi. Integrated solar still with an underground heat exchanger for clean water productions. *Journal of King Saud University - Engineering Sciences*, 32:339–345, 2020. doi:10.1016/j.jksues.2019.04.004.